Relative DOPA Deficiency in Lightly Pigmented Skin Contributes to UV-Independent Melanoma Susceptibility

Miriam Doepner[1], Christopher A. Natale[1], Todd W. Ridky[1]*

[1]Department of Dermatology, Perelman School of Medicine, University of Pennsylvania, Philadelphia, PA. USA

*Correspondence to: ridky@pennmedicine.upenn.edu

Abstract

Melanoma risk is higher for people with lightly pigmented skin (1:38) compared to those with darkly pigmented skin (1:1000). While this difference is typically attributed to the ultraviolet radiation (UVR) shielding effect of melanin pigment, here we show that other cell-intrinsic differences between dark and light MCs, independent of melanin and UV, regulate MC proliferative capacity, cellular differentiation state, and susceptibility to malignant transformation. These differences are driven by dihydroxyphenylalanine (DOPA), a melanin synthesis intermediate, and result from DOPA antagonism of the muscarinic acetylcholine receptor M_1 (CHRM1), a G Protein-Coupled Receptor (GPCR) expressed in MCs, but not previously known to bind DOPA, nor to affect melanoma pathobiology. Pharmacologic CHRM1 antagonism in melanoma leads to downregulation of c-Myc and FOXM1, both of which are proliferation drivers associated with aggressive melanoma. In preclinical melanoma models, pharmacologic CHRM1 inhibition *in vivo* inhibited melanoma growth. CHRM1 may be a new therapeutic target for melanoma.

Statement of Significance

A previously unrecognized ability of dihydroxyphenylalanine (DOPA) to inhibit the muscarinic acetylcholine receptor M_1 (CHRM1) in melanocytes contributes to decreased melanoma susceptibility in darkly pigmented skin, independent of ultraviolet exposure. Pharmacologic CHRM1 inhibition inhibits melanoma in preclinical melanoma models, indicating that CHRM1 may be a new therapeutic target for melanoma.

Introduction

Melanoma is the most lethal form of skin cancer and worldwide incidence is increasing. Despite advances in modern immune and targeted therapies, most patients with metastatic melanoma still die from their disease and new treatment approaches are needed.[1,2] Clues to new therapeutic approaches may lie in understanding the mechanisms by which melanoma differentially affects different populations of people. Here we consider why the lifetime risk for cutaneous melanoma is substantially higher for people with lightly pigmented skin compared to those with darkly pigmented skin, even when they live in the same geographic region and are thereby exposed to similar amounts of UVR.[3]

Melanoma develops from melanocytes (MCs), which normally reside in the basal layer of skin and hair follicles where they produce melanin pigment, the primary determinant of skin and hair color. Melanogenesis is a complex, multi-step process that begins with the non-essential amino acid L-tyrosine and results in the

production of mostly insoluble eumelanin (brown-black) or pheomelanin (red-yellow) polymers.[4–6] Variation in the eumelanin to pheomelanin ratio creates the natural diversity in human skin pigmentation. These baseline pigmentary differences result from numerous single nucleotide polymorphisms (SNPs) in at least 200 genes involved in melanin synthesis.[7] Eumelanin acts as a physical photoprotective filter against DNA damaging solar ultraviolet radiation (UVR) and thereby protects skin cells from deleterious mutations that may lead to malignant transformation.[8] While melanin's UVR shielding effect undoubtedly accounts for some of the difference of the lifetime melanoma risk, highly pigmented skin provides a sun protective factor (SPF) of only 2-3 versus lightly pigmented skin, which seems insufficient to completely explain the large difference in skin cancer incidence between people with lightly pigmented vs darkly pigmented skin.[9,10] Furthermore, a UVR shielding effect does not fully explain decades of epidemiologic data suggesting that there are UV-independent determinants of melanoma risk that also correlate with skin pigment type. Melanomas arising in completely sun-protected areas, such as anorectal melanoma, are 13-fold higher in people with lightly pigmented skin than those with darkly pigmented skin.[11,12] There is also an intriguing observation involving skin cancer in people from Africa with albinism. While affected individuals have epidermal MCs, they do not make melanin, and therefore have white or extremely lightly pigmented skin and hair. They exhibit photosensitivity and an expected elevated incidence of keratinocyte-derived cancers, including basal cell and squamous cell carcinomas. However, they appear highly resistant to melanoma suggesting that while their MCs are visibly light, they may be functionally "dark" with regard to melanoma, and thereby similar to those with darkly pigmented skin in their population group with shared African ancestry.[13,14] The mechanism(s) underlying these apparent UV-independent determinants of melanoma susceptibility are unknown.

Here, we show that dihydroxyphenylalanine (DOPA), a melanin synthesis intermediate, drives differentiation in primary human MCs, that is associated slower proliferation and resistance to the oncogenic effects of the major human melanoma oncoprotein BRAF(V600E). We show that DOPA functions to antagonize the muscarinic acetylcholine receptor M_1 (CHRM1), a G Protein-Coupled Receptor (GPCR), that is necessary and sufficient for DOPA's anti-proliferative effect. In preclinical melanoma models, pharmacologic CHRM1 inhibition *in vivo* inhibited melanoma growth, suggesting that CHRM1 antagonists may represent a previously unrecognized class of melanoma therapeutics.

Results

Darkly pigmented MCs are less tumorigenic than light pigmented MCs

Under standard cell culture conditions without UVR, lightly pigmented early passage primary human MCs (LMC) proliferated 2-3 times faster than darkly pigmented MCs (DMC) **(Figure 1A)**. Melanocyte proliferative capacity is classically inversely correlated with MC cellular differentiation state[15–19], which is primarily regulated by the activation of G_s-coupled G protein-coupled receptors (GPCRs).[20–23] Gs signaling stimulates production of cyclic adenosine monophosphate (cAMP) via adenylate cyclase. In MCs, cAMP activates protein kinase A (PKA), which phosphorylates and activates the cAMP response element-binding protein (CREB), which ultimately promotes downstream synthesis of proteins involved in melanin production, such as tyrosinase

(Tyr).[24,25] We examined whether the expression of proteins within this classic GPCR pathway differed between LMCs and DMCs. DMCs expressed lower levels of phosphorylated CREB (pCREB) and tyrosinase, as compared to light MCs **(Supplemental Figure 1A)**, suggesting that DMCs are more fully advanced along a cellular differentiation continuum that parallels the natural range of human skin pigment diversity. Consistent with this idea, DMCs expressed less of the stem cell marker and oncoprotein c-Myc **(Figure 1B, Supplemental Figure 1A).**

We hypothesized that these baseline differences in relative cellular differentiation state and proliferative capacity between DMCs and LMCs contribute to overall differential melanoma susceptibility. To test this *in vivo*, we used a genetically defined orthotopic human melanoma (heMel) model.[26,27] Primary LMC and DMCs were engineered via lentivirus to express mutant oncoproteins associated with spontaneous human melanoma including $BRAF^{V600E}$, dominant-negative $p53^{R248W}$, active $CDK4^{R24C}$, and hTERT[26]. Equal expression of all oncoproteins was confirmed in darkly pigmented and lightly pigmented heMel cells **(Supplemental Figure 1C).** The proliferation and differentiation differences between DMCs and LMCs observed in the untransduced parental cells remained after transduction of the oncoproteins. Darkly pigmented heMel cells proliferated over two times slower than lightly pigmented heMel cells and maintained their more differentiated phenotype **(Figure 1C, Supplemental Figure 1B)**, suggesting that cell intrinsic factors in DMCs may protect them from the oncogenic effects of common melanoma drivers. To test whether these *in vitro* differences translated to different melanoma phenotypes *in vivo*, lightly and darkly pigmented heMel cells were combined with primary human keratinocytes and incorporated into devitalized human dermis to establish 3-dimensional skin tissues in organotypic culture.[28] We then grafted the engineered skin onto the orthotopic location on the backs of female severe combined immunodeficient (SCID) mice. After 100 days, the grafts were harvested and analyzed histologically. Tissues with lightly pigmented heMel cells formed early melanomas, with large proliferative melanocytic nests with hallmark melanoma features, including early dermal invasion and upward Pagetoid scatter **(Figure 1D, E).** In striking contrast, darkly pigmented heMel cells did not progress to melanoma, although the individual heMel cells were present in the tissues **(Figure 1D, E).** These results show that DMCs resist BRAF-driven transformation, independent of UVR.

Endogenously synthesized DOPA inhibits MC proliferation

To begin defining the mechanism(s) responsible for limiting proliferation and oncodriver responses in DMCs, we first examined components of the melanin synthesis pathway. Because melanin itself is a largely insoluble heterogeneous polymer without known signaling activity, we looked to upstream melanin synthetic intermediates. Melanin is synthesized via a complex multistep process involving serial oxidation and polymerization of tyrosine and is regulated by over 200 different genes **(Figure 2A)**.[29] Tyrosine is first converted into L-dihydroxyphenylalanine (DOPA) via tyrosinase, and this is the rate limiting enzyme of melanin synthesis.[23,30] Consistent with the premise that tyrosinase activity increases in parallel with eumelanin content across the human pigment spectrum[6], we detected approximately 300% more DOPA in cultures of primary human DMCs, as compared to LMCs **(Figure 2B).**

To test whether DOPA inhibits MC proliferation, we exposed LMC and DMCs to increasing concentrations of DOPA. DOPA decreased proliferation of LMCs in a dose-responsive and saturable manner, strongly suggesting a specific receptor mediated activity. In contrast, DOPA had no effect on proliferation of DMCs. DOPA effects in LMCs saturated at 6.25 μM. At this exposure, LMCs proliferate at the same rate as DMCs, suggesting that DMCs contain a saturating amount of endogenously synthesized DOPA **(Figure 2C).** Consistent with this, exogenous DOPA increased melanin synthesis in LMCs, but did not have any effect on melanin content in DMCs **(Supplemental Figure 1A).**

To test whether the anti-proliferative effect of DOPA is dependent on melanin synthesis, we utilized the tyrosinase inhibitor N-phenylthiourea (PTU).[31–33] As tyrosinase catalyzes not only the reaction of tyrosine to DOPA, but also the subsequent conversion of DOPA to dopaquinone **(Figure 2A)**, PTU prevents conversion of exogenous DOPA to melanin. In LMCs, PTU alone had no significant effect on proliferation, while the combination of PTU and DOPA continued to inhibit cell growth **(Figure 2D, Supplemental Figure 2B).** In DMCs, PTU decreased pigment production and increased proliferation rate, however DMCs treated with both PTU and DOPA proliferated at the slow baseline DMC rate, despite the fact that they remained lightly pigmented **(Figure 2E).** Together, these data show that DOPA's effects on MC proliferation are independent of melanin synthesis, and that differences in endogenously produced DOPA are likely responsible for most, if not all, of the observed proliferation differences between DMCs and LMCs.

In addition to melanin, the biologic impact of DOPA is also generally attributed to its conversion to dopamine and 3-O-methyldopa (**Figure 2A**), both of which affect activity of dopamine receptors. However, neither of these DOPA metabolites appeared necessary for the anti-proliferative effects of DOPA in MCs. We used the DOPA decarboxylase (DDC) inhibitor, carbidopa, to inhibit the conversion of DOPA to dopamine, and the catechol-O-methyltransferase (COMT) inhibitor, entacapone, to block synthesis of 3-O-methyldopa. Neither inhibitor altered the anti-proliferative effect of DOPA **(Supplemental Figure 2C-E).** Also consistent with the idea that dopamine is not a mediator of the observed DOPA effects, LC/mass spectrometry analysis did not detect any dopamine in MCs (although we readily detected DOPA in the same samples). To analyze if DOPA impacted other primary cells found in skin, we treated primary human fibroblasts, keratinocytes, and melanocytes with increasing concentrations of DOPA. We observed no effect to primary human keratinocytes, and mild inhibition of fibroblast growth **(Supplemental Figure 2F).** To test whether melanoma cells also respond to DOPA, we treated multiple human and mouse melanoma cell lines with DOPA/carbidopa and observed marked inhibition of proliferation in most melanoma lines, independent of BRAF and NRAS mutational status **(Figure 2F, Supplementary Table 1).**

DOPA antagonizes CHRM1

Data in Figure 1 and 2 strongly suggest that DOPA effects in MCs and melanoma cells are specific and receptor mediated. To identify the receptor(s) responsible, we first considered GPCRs, as melanin synthesis in MCs is classically regulated by the melanocortin receptor MC1R, a G_s-coupled GPCR. To our knowledge, the only previous report associating DOPA with a specific receptor in any cell type identified ocular albinism type 1

(OA1) as a possible DOPA receptor in retina pigment epithelial cells.[34] To test whether OA1 mediated DOPA effects in melanoma, we depleted OA1 in DOPA sensitive human melanoma cells using siRNA. This had no effect on the DOPA response **(Supplemental Figure 3A).** To identify new possible GPCR candidates, we used PRESTO-TANGO screening, to test whether DOPA bound to any of approximately 320 nonolfactory human GPCRs.[35] We compared top hits against whole transcriptome melanocyte RNAseq data and identified 8 GPCRs predicted to be activated by DOPA, and 9 GPCRs predicted to be inhibited by DOPA **(Figure 3A).** These top hits were validated via pooled siRNA knockdown of each GPCR receptor in A375 melanoma cells. The only siRNA pool that rendered cells insensitive to DOPA was the pool targeting the cholinergic receptor muscarinic 1 (CHRM1), a G_q coupled GPCR **(Figure 3B,C, Supplemental Figure 3A,B).** To verify results seen with siRNA, we utilized a complementary CRISPR-Cas9 gene editing approach with guide RNAs targeting CHRM1 in A375 melanoma cells. While we were unable to achieve full knockout of CHRM1, potentially due to the hypotriploid karyotype of this model, CRISPR-Cas9 CHRM1 knockdown nonetheless markedly inhibited the antiproliferative effects of DOPA/carbidopa **(Figure 3D, Supplemental Figure 3C).** Consistent with these data showing that CHRM1 mediates DOPA effects, DOPA responses in melanoma cell lines correlated with CHRM1 expression **(Figure 3E)**. CHRM1 has not previously been shown to bind to DOPA, nor to affect melanoma pathobiology, but CHRM1 has been implicated in prostate cancer progression.[36–38] While CHRM1 has not previously been reported in melanoma, previous reports have shown the muscarinic receptor family is present in normal human melanocytes.[39] As DOPA appeared to function as a CHRM1 antagonist, we next tested whether the known CHRM1 synthetic antagonist, pirenzepine[40,41], mimics the observed DOPA effects. In a dose dependent manner, pirenzepine recapitulated the anti-proliferative effects of DOPA/carbidopa treatment in A375 human melanoma, but not WM2664, as these cells do not express CHRM1. In contrast, the CHRM1 agonist, pilocarpine[42,43], had opposite effects, and promoted proliferation in both melanoma cells and DMCs **(Supplemental Figure 3D-F).** Together these data show that CHRM1 promotes MC and melanoma cell proliferation, that CHRM1 is necessary for the anti-proliferative effects of DOPA.

To determine if CHRM1 expression is sufficient to confer DOPA sensitivity to DOPA insensitive melanoma cells lacking CHRM1, we used lentiviral transduction to express CHRM1 in two non-responding melanoma cell lines, RPMI-7951 and WM2664. Upon CHRM1 expression, cells grew faster than parental controls, suggesting that CHRM1 may function as a melanoma oncodriver **(Figure 3F,G).** Importantly, CHRM1 expression rendered RPMI-7951 and WM2664 newly sensitive to DOPA, supporting the idea that CHRM1 is both necessary and sufficient for DOPA effects in MC and melanoma. To further confirm the specificity of these genetic and pharmacologic data, and to control for possible off target effects of the CHRM1 targeting gRNA, we used lentiviral transduction to restore CHRM1 expression in A375 cells in which we had previously depleted CHRM1 using CRISPR-Cas9. With this transgene rescue, cells were resensitized to DOPA **(Supplemental Figure 4A,B).** Together, these data show that CHRM1 is the major mediator of DOPA effects in melanoma.

DOPA inhibits oncogenic Gq signaling

CHRM1 is a Gq coupled GPCR known to activate both Ras/MAPK and PI3K/Akt signaling in other cells types.[38,44,45] Both of these pathways are major drivers of melanoma and other cancers, and targets of approved inhibitors used clinically.[46–49] Consistent with our discovery that CHRM1 is a DOPA sensitive melanoma driver, exogenous DOPA induced rapid depletion of both phosphorylated extracellular-signal-regulated kinase (ERK), and phosphorylated AKT in melanoma cells **(Supplemental Figure 5A).** We also noted parallel depletion of both c-Myc and FOXM1, which both function as transcription factors and proliferation drivers positively regulated by MAPK and AKT [50–54] **(Figure 4A,B).** Importantly, we also found that light melanocytes with less endogenous DOPA express higher levels of FOXM1 at baseline, as compared to dark melanocytes **(Figure 4C).**

We were specifically interested in the downregulation of FOXM1, as FOXM1 is overexpressed in up to 70% of metastatic melanomas and correlates with worse outcomes.[51,55,56] FOXM1 stimulates cell growth by promoting genes critical for cell proliferation and is a key regulator of the G1-S phase transition, and small molecule FOXM1 inhibitors are available for *in vitro* studies.[53,54,57]

To test whether FOXM1 loss was necessary for the anti-proliferative effects of DOPA, we overexpressed FOXM1C, the primary isoform in melanocytes and melanoma.[51] This partially inhibited DOPA/carbidopa's anti-proliferative effect **(Figure 4C,D).** We next tested whether human melanocytes and melanoma cells responded to the FOXM1 inhibitor FDI-6[57]. In vitro exposure to FDI-6 inhibited melanoma cell proliferation and, most strikingly, included a dramatic change melanoma cell morphology: cells became multipolar and larger, and generally appeared more like normal primary melanocytes than the untreated melanoma cells **(Figure 4F,G, Supplemental Figure 5B).** These morphologic features have also been recognized by others as indicative of a more fully differentiated melanocyte cell state.[58,59] Consistent with this idea, LMCs were more sensitive to FDI-6 treatment than DMCs **(Supplemental Figure 5C)**.

DOPA inhibits melanoma *in vivo*.

As DOPA antagonism of CHRM1 inhibited FOXM1 and the MAPK and AKT pathways, all of which promote melanoma, we next questioned whether DOPA may have therapeutic utility as a systemically delivered agent for melanoma *in vivo*. Systemic delivery of combined L-DOPA and carbidopa is already FDA-approved for Parkinson's disease[60]. The DOPA/carbidopa combination is utilized, rather than DOPA alone, because carbidopa inhibits DDC and thereby prevents DOPA from being converted to dopamine everywhere except the brain, where it is needed to treat Parkinson's: carbidopa does not cross the blood brain barrier, whereas DOPA does. This combination is therefore ideal for our purposes, because we wanted to expose the subcutaneous melanomas to DOPA, not to dopamine. BL/6 mice harboring syngeneic YUMM1.7 melanoma (*Braf*$^{V600E/wt}$*Pten*$^{-/-}$ *Cdkn2*$^{-/-}$) were treated with a combination of 300 mg/kg L-DOPA methyl ester and 75 mg/kg carbidopa. Treatment was initiated after tumors reached 3-4 mm in diameter **(Figure 5A).** DOPA/carbidopa treatment was well tolerated by mice and significantly inhibited YUMM1.7 tumor growth **(Figure 5B).** Together, these

results show that combination DOPA/carbidopa treatment, an FDA approved therapy for Parkinson's disease, might potentially be repurposed as a melanoma therapeutic.

Discussion

Decades of clinical and epidemiological data suggest that the physical UV shielding effect of melanin does not fully explain the difference in melanoma incidence between lightly and darkly pigmented skin. We hypothesized that the mechanisms responsible for this also contribute to the differences in proliferation rate that we routinely observe between LMC and DMCs. To our knowledge, this is the first work to directly explore the mechanism responsible for these differences, to show that CHRM1 is a DOPA receptor, to show that CHRM1 affects melanocyte homeostasis, and to demonstrate that CHRM1 is a potential therapeutic target for melanoma. Future research utilizing melanocytes should consider for these baseline differences in DOPA and CHRM1 signaling, and how they may affect observed phenotypes and drug sensitivity.

Our data are consistent with some provocative, but mechanistically unexplained findings from older literature. DOPA was shown 28 years ago to bind to a protein in rodent melanoma cell membranes although the specific protein was not identified, and the functional consequences of that binding for MC function or melanoma pathology were not determined.[61,62] Additionally, studies have identified L-DOPA as a regulator of melanocyte functions, albeit direct mechanism(s) were not established.[63,64] Even more tantalizing, 43 years ago, L-DOPA methyl ester was shown to inhibit B16 melanoma in mice, but whether that resulted from DOPA itself, melanin, or other metabolite, was the mechanism(s) responsible were not determined, and this discovery appears to be mostly forgotten in recent melanoma literature[65–70].

Acetylcholine signaling through the muscarinic acetylcholine receptors (mAChRs), including CHRM1, ultimately impacts a wide spectrum of diseases, and many mAChRs antagonists are already approved in the U.S for use in people. Among these are atropine for childhood myopia[71] and scopolamine for motion sickness[72]. Unfortunately, these agents have very short half lives in vivo, and are thereby not suitable for cancer studies. Nonetheless, we have shown that future mAChR antagonists with improved systemic pharmacokinetic properties may be effective against melanoma.

Cholinergic muscarinic receptors are best known for their activity in the nervous system, and recent work in murine prostate cancer models established that the nerves activate pro-tumorigenic cholinergic signaling in the tumor microenvironment that promotes tumor invasion and metastasis.[37] As the skin is heavily innervated, and there are physical connections between epidermal melanocytes, it seems possible that nerve derived factors may similarly promote melanoma.[73]

We showed that combination treatment of DOPA and carbidopa, an FDA approved therapy for Parkinson's disease, mimics the effects of endogenously produced DOPA in DMCs, and thereby inhibits melanoma. Parkinson's disease is a neurodegenerative disorder caused by a loss of neurons in the substantia nigra, ultimately leading to dopamine deficiency that quickly leads to a decline in motor function.[74] Multiple epidemiological studies have found an association between melanoma and Parkinson's disease melanoma.[75–77] This association is reciprocal: patients with melanoma have an increased risk of Parkinson's disease and

patients with Parkinson's disease are more likely to develop melanoma. Further, studies have also shown that incidence in Parkinson's disease is 2-3 times more common in white populations as compared to African-American populations,.[78–80] These epidemiological studies, together with this current work, suggest that the relative lack of DOPA in lightly pigmented individuals may predispose them not only to melanoma, but also Parkinson's; however, the pathobiology of Parkinson's disease is complex and further investigation is needed to determine whether these two seemingly disparate diseases are mechanistically linked through DOPA.

Finally, we established that pharmacologic DOPA/carbidopa led to decreases in activation of both the MAPK and AKT pathways and ultimately downregulation of FOXM1, a major cancer driver.[56,81] While FOXM1 is downstream of both the MAPK and AKT pathways, FOXM1 depletion is unlikely to be the sole mechanism by which DOPA inhibits melanoma as FOXM1 overexpression only partially rescued cell proliferation in the face of exogenous DOPA. However, selective pharmacologic FOXM1 inhibition significantly reduced melanoma cell growth and increased differentiation, suggesting another new potential therapeutic melanoma target. While FDI-6 shows promising results *in vitro* and is a useful and readily available research compound, it is not stable *in vivo.* However, a new class of FOXM1 inhibitors with more favorable pharmacokinetic properties were recently shown to have activity in preclinical breast cancer models.[82] Future studies will be needed to see if their utility extends to melanoma and other cancers.

Together, this work demonstrates how the natural genetic diversity in people can be used as a window to discover new signaling pathways regulating normal tissue homeostasis and carcinogenesis.

Methods

Cell culture and proliferation assays

Primary human melanocytes, keratinocytes, and fibroblasts were extracted from fresh discarded human foreskin and surgical specimens as previously described.[28,83–85] Keratinocytes were cultured in a 1:1 mixture of Gibco Keratinocytes-SFM medium + L-glutamine + EGF + BPE and Gibco Cascade Biologics 154 medium with 1% penicillin-streptomycin (Thermo Fisher Scientific. # 15140122). Fibroblasts were cultured in DMEM (Mediatech, Manassas, VA, USA) with 5% FBS (Invitrogen, Carlsbad, CA, USA) and 1% Penicillin-Streptomycin. Primary melanocytes and human-engineered melanoma cells (heMel) were cultured in Medium 254 (ThermoFisher, #M254500) with 1% penicillin-streptomycin.

YUMM1.7, SH-4 and SK-MEL-2 cells were purchased from ATCC (YUMM1.7 ATCC® CRL-3362™; SH-4 ATCC® CRL-7724™; SK-MEL-2 ATCC® HTB-68™) and cultured in DMEM with 5% FBS and 1% Penicillin-Streptomycin. SK-MEL-3 cells were purchased from ATCC (ATCC® HTB-69™ and cultured in McCoy's 5A (Modified) Medium with 15% FBS (Invitrogen, Carlsbad, CA, USA) and 1% Penicillin-Streptomycin. RPMI-7951 and SK-MEL-24 cells were purchased from ATCC (RPMI-7951 ATCC® HTB-66™; ATCC® HTB-71™) and cultured in Eagle's Minimum Essential Medium with 15% FBS and 1% Penicillin-Streptomycin. WM46 and WM2664 melanoma cells were a gift from Meenhard Herlyn (Wistar Institute, Philadelphia, PA, USA) and were

cultured in TU2% media. Tumor cells were regularly tested using MycoAlert Mycoplasma Detection Kit from Lonza (Allendale, NJ, USA).

For monitoring cell proliferation $10x10^5$ YUMM1.7 or A375, $12x10^5$ RPMI-7951, $15x10^5$ WM46, WM2664, SH4, SK-MEL-2, SK-MEL-24, SK-MEL-3, or $30x10^5$ melanocytes were seeded per well in 12-well cell culture plates. Cells were treated every second day and manually counted in triplicate using a hemocytometer. All the experiments were performed in cell populations that were in culture during a maximum of 3 weeks (5 passages in average) since thaw from the corresponding stock.

3,4-Dihydoxy-L-phenylalanine (D9628), N-Phenylthiourea (P7629), and FDI-6 (SML1392) were purchased from Sigma-Aldrich (St. Louis, MO, USA). (S)-(-)-Carbidopa (0455), Pirenzepine dihydrocholoride (1071), Pilocarpine hydrocholride (0694) were purchased from Tocris Bioscience (Bristol, United Kingdom). 3-O-methyl-L-DOPA hydrate (20737) and Entacapone (14153) were purchased from Cayman Chemicals (Ann Arbor, MI, USA).

Genetic manipulation of CHRM1

We used lentiviral transduction to deliver dox-inducible Cas9 and gRNA targeting CHRM1 in human A375 melanoma cells. Three different guide RNAs were used to target CHRM1. Transduced cells were selected with puromycin, and single cells subsequently isolated, expanded and examined for CHRM1 protein expression, compared to clones isolated in parallel with no doxycycline treatment. The following gRNA sequences were used (5'-3'):

sgCHRM1.1_Fw: caccgGCTCCGAGACGCCAGGCAAA
sgCHRM1.1_Rv: aaacTTTGCCTGGCGTCTCGGAGCc
sgCHRM1.2_Fw: caccgGATGCCAATGGTGGACCCCG
sgCHRM1.2_Rv: aaacCGGGGTCCACCATTGGCATCc
sgCHRM1.3_Fw: caccgCAAGCGGAAGACCTTCTCGC
sgCHRM1.3_Rv: aaacGCGAGAAGGTCTTCCGCTTGc

Using ThermoFisher's Silencer Silect protocol, we knocked down CHRM1 in human A375 melanoma cells. Briefly, each siRNA was diluted in Opti-MEM medium (Invitrogen, 31985062) to a concentration of 10 μM, to ultimately be diluted to 30 pmol in a 6-well plate. If siRNA were pooled, each individual siRNA was used at 10 pmol (for a combined total of 30 pmol) in a 6-well plate. Diluted siRNA's were combined with diluted Lipofectmaine (Invitrogen, 11668027) and incubated on cells for 24 hours. After 24 hours cells were plated in a 12 well plate with 10,000 cells per well and treated with a combination of DOPA and carbidopa for four days. We used three different siRNA against CHRM1: s3023 (labeled siCHRM1.1), s3024 (labeled siCHRM1.2), s553080 (labeled siCHRM1.3). Negative controls included Negative Control No.1 (ThermoFisher, 4390843)

and Negative Control No. 2 (ThermoFisher, 4390846) and a positive control against Kif11 (University of Pennsylvania, High-throughput sequencing core).

Human-engineered melanoma xenografts

Organotypic skin grafts were established using modifications to previously detailed methods.[19,28] The Keratinocyte Growth Media (KGM) used for keratinocyte-only skin grafts was replaced with modified Melanocyte Xenograft Seeding Media (MXSM). MXSM is a 1:1 mixture of KGM, lacking cholera toxin, and Keratinocyte Media 50/50 (Gibco) containing 2% FBS, 1.2 mM calcium chloride, 100 nM Et-3 (endothelin 3), 10 ng/mL rhSCF (recombinant human stem cell factor), and 4.5 ng/mL r-basic FGF (recombinant basic fibroblast growth factor). Briefly, primary human melanocytes were transduced with lentivirus carrying BRAF(V600E), dominant-negative p53(R248W), active CDK4(R24C) and hTERT. Transduced melanocytes (1×10^5 cells) and keratinocytes (5×10^5 cells) were suspended in 80 µL MXSM, seeded onto the dermis, and incubated at 37˚C for 4 days at the air–liquid interface to establish organotypic skin. Organotypic skin tissues were grafted onto 5–7-week-old female ICR SCID mice (Taconic) according to an IACUC–approved protocol at the University of Pennsylvania. Mice were anesthetized in an isoflurane chamber and murine skin was removed from the upper dorsal region of the mouse. Organotypic human skin was reduced to a uniform 11 mm × 11 mm square and grafted onto the back of the mouse with individual interrupted 6–0 nylon sutures. Mice were dressed with Bactroban ointment, Adaptic, Telfa pad, and Coban wrap. Dressings were removed 2 weeks after grafting. Mice were sacrificed 100 days after grafting and organotypic skin was removed for histology.

Subcutaneous tumors and treatments

All mice were purchased from Taconic Biosciences, Inc. (Rensselaer, NY, USA). These studies were performed without inclusion/exclusion criteria or blinding but included randomization. Based on a two-fold anticipated effect, we performed experiments with at least 5 biological replicates. All procedures were performed in accordance with International Animal Care and Use Committee (IACUC)-approved protocols at the University of Pennsylvania. Subcutaneous tumors were initiated by injecting 10×10^5 YUMM1.7 cells in 50% Matrigel (Corning, Bedford, MA, USA) into the subcutaneous space on the left and right flanks of mice. L-DOPA methyl ester (300 mg/kg, Tocris # 0455) and carbidopa (75 mg/kg, Cayman #16149) were injected intraperitoneally daily for three weeks, then five days on, 2 days off for the remainder of the experiment. Both drugs were resuspended in normal saline. Adhering to previous literature[86,87], carbidopa was injected one hour before L-DOPA injection. As subcutaneous tumors grew in mice, perpendicular tumor diameters were measured using calipers. Volume was calculated using the formula $L \times W^2 \times 0.52$, where L is the longest dimension and W is the perpendicular dimension. Animals were euthanized when tumors exceeded a protocol-specified size of 15 mm in the longest dimension. Secondary endpoints include severe ulceration, death, and any other condition that falls within the IACUC guidelines for Rodent Tumor and Cancer Models at the University of Pennsylvania.

Western blot analysis

Adherent cells were washed once with DPBS, and lysed with 8M urea containing 50 mM NaCl and 50 mM Tris-HCl, pH 8.3, 10 mM dithiothreitol, 50 mM iodoacetamide. Lysates were quantified (Bradford assay), normalized, reduced, and resolved by SDS gel electrophoresis on 4–15% Tris/Glycine gels (Bio-Rad, Hercules, CA, USA). Resolved protein was transferred to PVDF membranes (Millipore, Billerica, MA, USA) using a Semi-Dry Transfer Cell (Bio-Rad), blocked in 5% BSA in TBS-T and probed with primary antibodies recognizing β-Actin (Cell Signaling Technology, #3700, 1:4000, Danvers, MA, USA), c-Myc (Cell Signaling Technology, #5605, 1:1000), p-RB (Cell Signaling Technology, #8516, 1:1000), RB (Cell Signaling Technology, #9313, 1:1000), p-CREB (Cell Signaling Technology, #9198, 1:1000), CREB (Cell Signaling Technology, #9104, 1:1000), tyrosinase (Abcam, T311, 1:1000), p53 (Cell Signaling Technology, #2527, 1:1000), CDK4 (Cell Signaling Technology, #12790, 1:1000), P-ERK (Cell Signaling Technology, Phospho-p44/42 MAPK (Erk1/2) (Thr202/Tyr204) (D13.14.4E) XP® Rabbit mAb #4370. 1:1000), ERK (Cell Signaling Technology, p44/42 MAPK (Erk1/2) (137F5) Rabbit mAb #4695, 1:1000), pAKT S473 (Cell Signaling Technology, #9271, 1:1000), AKT (Cell Signaling Technology, #9272, 1:1000) CHRM1 (Invitrogen, #PA5-95151, 1:1000), FoxM1 (Cell Signaling Technology, #5436, 1:1000). After incubation with the appropriate secondary antibody, proteins were detected using either Luminata Crescendo Western HRP Substrate (Millipore) or ECL Western Blotting Analysis System (GE Healthcare, Bensalem, PA). After incubation with the appropriate secondary antibody [(Rabbit Anti-Mouse IgG H&L (Biotin) preabsoFS9rbed (ab7074); Anti-mouse IgG, HRP-linked Antibody #7076. 1:2000)] proteins were detected using ClarityTM Western ECL Substrate (Bio-Rad. #170-5060). All western blots were repeated at least 3 times.

Quantitative RT-PCR

RNA was extracted using RNeasy kit (Qiagen. #74104) following the manufacturer's instructions. cDNA was obtained using High Capacity cDNA Reverse Transcription Kit (Applied Biosystems #4368814). For quantitative real-time PCR, PowerUP™ SYBR™ Green Master Mix (Applied Biosystems #A25741) was used. ViiA 7 Real-Time PCR System was used to perform the reaction (Applied Biosystems). Values were corrected by b-actin expression. The $2^{-\Delta\Delta Ct}$ method was applied to calculate the relative gene expression. Primers used are included in Table S2.

PRESTO-TANGO

We used the National Institute of Mental Health's Psychoactive Drug Screening Program at the University of North Carolina to perform PRESTO-TANGO[35] analysis of 400 non-olfactory GPCRs in the presence or absence of L-DOPA.

Immunohistochemistry and quantification

Formalin-fixed paraffin-embedded (FFPE) human skin tissue sections from organotypic tissue was stained for MITF (NCL-L-MITF, Leica Biosystems, Nussloch, Germany), MelanA (NCL-L-MITF, Leica Biosystems), and

Ki67 (NCL-L-Ki67-MM1, Leica Biosystems). Staining was performed following the manufacturer's protocol for high temperature antigen unmasking technique for paraffin sections. For melanin staining, FFPE embedded tissue was subjected to Fontana-Masson histochemical stain as previously described.[19,88]

Tissue section quantification was performed according to Billings et al. (2015). Briefly, 10X photomicrograph images of representative tissue sections were taken using the Keyence BZ-X710 (Itasca, IL, USA). Tiff files of the images were saved and transferred to FIJI (Image J). Images corresponding to the single specific color were then analyzed to determine the number of pixels in each sample and normalized to epidermal area. The numbers of pixels representing Melan-A staining were normalized to the total amount of epidermal area.

HPLC-MS

We used the Metabolomics Core at the Children's Hospital of Philadelphia (https://www.research.chop.edu/metabolomic-core) to perform HPLC for DOPA in lightly and darkly pigmented melanocytes. Cells were scraped from tissue culture plates, resuspended in 4% perchloric acid (PCA), and immediately brought to core.

Melanin assay

Cells (1×10^5) were seeded uniformly on 6-well tissue culture plates. Cells were treated with vehicle controls, DOPA, or PTU for 7 days. Cells were then trypsinized, counted, and pellets containing 300,000 cells were spun at 300 g for 5 min. The cell pellets were solubilized in 120 µL of 1M NaOH, and boiled at 100C for 5 min. The optical density of the resulting solution was read at 450 nm using an Emax microplate reader (Molecular Devices, Sunnyvale, CA, USA). The absorbance was normalized to a control pellet of 300,000 WM46 cells. All melanin assays were repeated at least three times and each time performed in triplicate.

Statistical analysis

All statistical analysis was performed using Graphpad Prism 8 (Graphpad Software, La Jolla, CA, USA). No statistical methods were used to predetermine sample size. Details of each statistical test used are included in the figure legends.

Acknowledgements

GPCR functional data was generously provided by the National Institute of Mental Health's Psychoactive Drug Screening Program, Contract # HHSN-271-2018-00023-C (NIMH PDSP). The NIMH PDSP is Directed by Bryan L. Roth MD, PhD at the University of North Carolina at Chapel Hill and Project Officer Jamie Driscoll at NIMH, Bethesda MD, USA.

Figure Legends

Figure 1: Cell-intrinsic differences render DMCs less tumorigenic than LMCs

(A) Scatter plot of primary human melanocytes based on the relative melanin intensity at 450 nm wavelength plotted and proliferation capacity. (B) Western blot of proliferation markers lightly pigmented melanocytes (LMC) and darkly pigmented melanocytes (DMC) at baseline. (C) Scatter plot of transformed human engineered melanoma (heMel) based on the relative melanin intensity at 450 nm wavelength plotted and proliferation capacity. (D) Quantification of positive epidermal MITF staining area compared to total epidermal area in LMC and DMC heMel samples. (E) Histologic characterization of representative orthotopic skin and resulting tumors, including melanocyte and proliferation markers MITF, Ki67/MART, and Fontana Masson (Melanin). Images taken at 20x magnification. Scale bar set at 100 μm.

Figure 2: Endogenously synthesized DOPA inhibits MC proliferation

(A) Schematic diagram depicting melanin synthesis. Red text denotes pharmacologic inhibitors used to block enzymatic conversions. (B) LC-MS for DOPA in lightly pigmented melanocytes (LMC) and darkly pigmented melanocytes (DMC). (C) Dose curve of L-DOPA in representative LMC and DMC after 4 days treatment. (D) Light melanocytes treated with either 25 μM L-DOPA, 75 μM phenylthiourea (PTU), or a combination. P-value *** = 0.0001, **** < 0.0001. (E) Dark melanocytes treated with either 25 μM L-DOPA, 75 μM phenylthiourea (PTU), or a combination. P-value **** = 0.0006. (F) (G) Panel of melanoma cell lines treated with combination 25 μM L-DOPA and 6.25 μM carbidopa.

Figure 3: DOPA antagonizes CHRM1

(A) Log-fold activation or inhibition of the PRESTO-Tango DOPA receptor. Data points shaded based on RNA-sequencing expression data of melanocytes (FPKM). (B) siRNA against CHRM1 in A375 human melanoma in the presence of 25 μM L-DOPA and 6.25 μM carbidopa after 5 days treatment. (C) qPCR for CHRM1 of siRNA in A375 confirming knockdown. Timepoint taken 24 hours after siRNA transfection. (D) CRISPR-Cas9 guides targeting CHRM1 in A375 human melanoma in the presence of 25 μM L-DOPA and 6.25 μM carbidopa after 5 days. (E) Low CHRM1 expression via qPCR correlates with lack of response to 25 μM L-DOPA and 6.25 μM carbidopa. (F) CHRM1 overexpression in WM2664 and RPMI-7951 human melanoma (DOPA non-responders) in the presence or absence of 25 μM L-DOPA and 6.25 μM carbidopa after 5 days treatment. (G) Western blot for CHRM1 in WM2664 and RPMI-7951 with either empty vector or CHRM1 overexpression.

Figure 4: DOPA inhibits oncogenic Gq signaling

(A) Western blot of short-term time course in A375 human melanoma treated with 25 μM L-DOPA and 6.25 μM carbidopa. (B) FOXM1 RNA-level via qPCR of time-course in A375 human melanoma treated with 25 μM L-DOPA and 6.25 μM carbidopa. (C) Western blot of FOXM1 and c-Myc at baseline in light and dark melanocytes. (D) Overexpression of FOXM1C versus empty vector in A375 human melanoma treated with 25 μM L-DOPA and 6.25 μM carbidopa. (E) Western blot confirming FOXM1C overexpression in A375 human melanoma. (F) 24 hour treatment of A375 human melanoma, lightly pigmented melanocytes (LMC), and darkly

pigmented melanocytes (DMC) with increasing concentrations of FDI-6 (FOXM1i). (G) Change in number of dendrites after 24 hour treatment in A375 human melanoma with FDI-6 (FOXM1i).

Figure 5: DOPA inhibits melanoma *in vivo*.

(A) Experimental timeline of combination DOPA and carbidopa treatment of human melanoma cells, n=5 per group. (B) Tumor growth over time of mice treated with vehicle or 300 mg/kg L-DOPA methyl ester and 75 mg/kg carbidopa. P-value ** = 0.0065.

Figure 1.

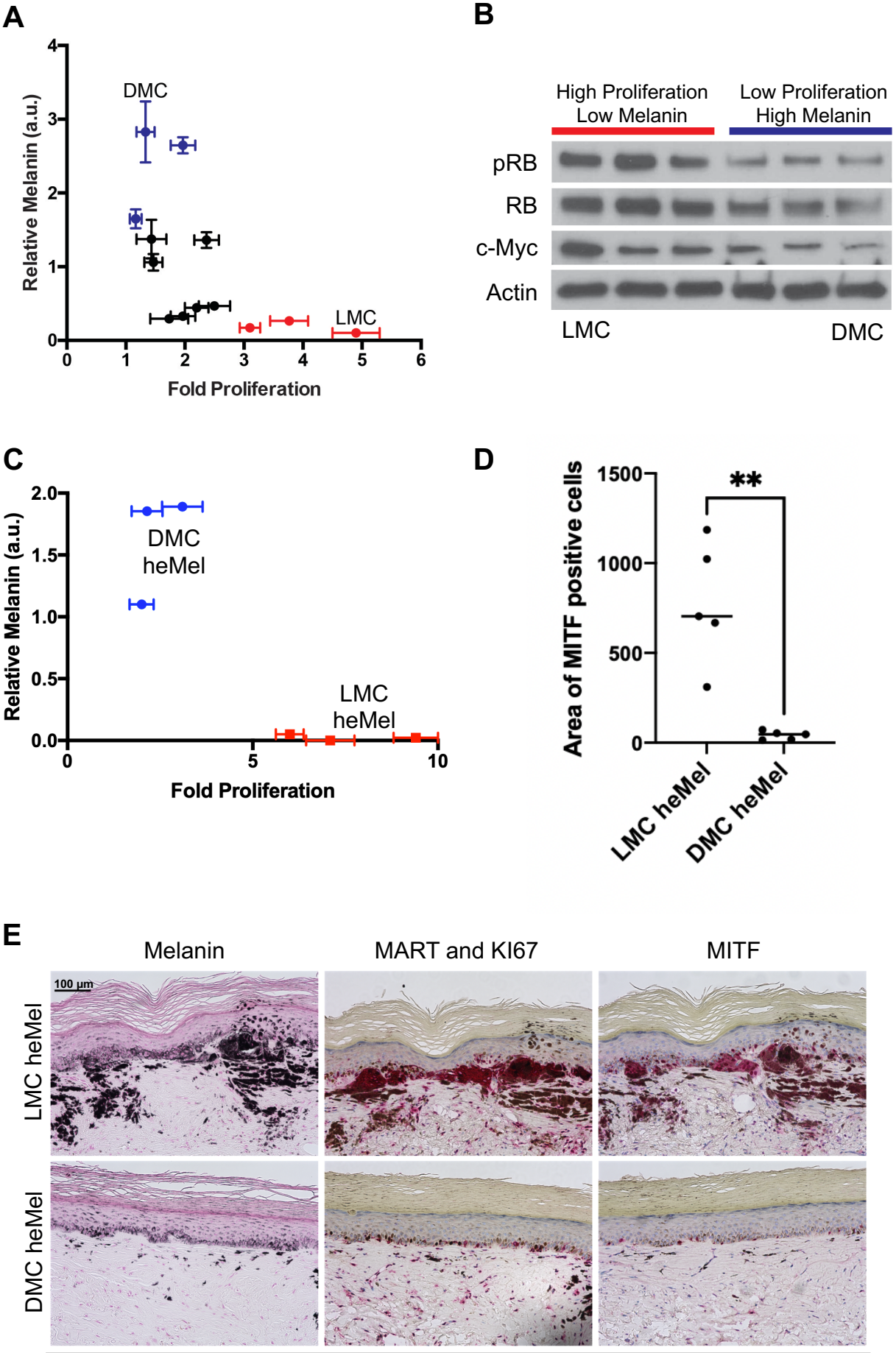
A
Relative Melanin (a.u.)
Fold Proliferation
DMC
LMC
B
High Proliferation
Low Melanin
Low Proliferation
High Melanin
pRB
RB
c-Myc
Actin
LMC
DMC
C
Relative Melanin (a.u.)
Fold Proliferation
DMC
heMel
LMC
heMel
D
Area of MITF positive cells
**
LMC heMel
DMC heMel
E
Melanin
MART and KI67
MITF
100 µm
LMC heMel
DMC heMel

Figure 2.

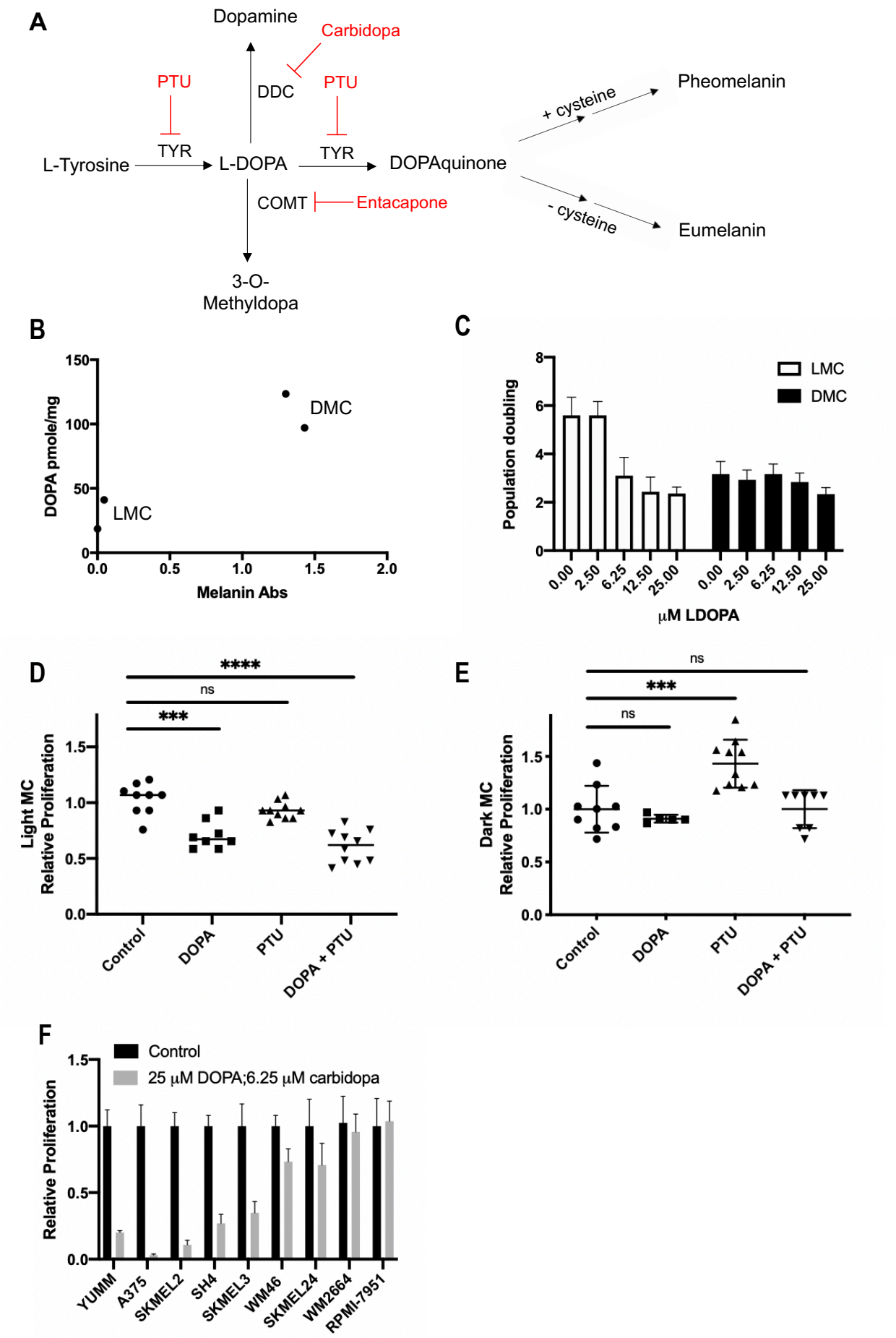
A
Dopamine
Carbidopa
PTU
DDC
PTU
TYR
TYR
L-Tyrosine
L-DOPA
DOPAquinone
+ cysteine
Pheomelanin
- cysteine
Eumelanin
COMT
Entacapone
3-O-Methyldopa
B
DOPA pmole/mg
Melanin Abs
DMC
LMC
C
Population doubling
LMC
DMC
μM LDOPA
D
Light MC Relative Proliferation
Control
DOPA
PTU
DOPA + PTU
E
Dark MC Relative Proliferation
Control
DOPA
PTU
DOPA + PTU
F
Relative Proliferation
Control
25 μM DOPA;6.25 μM carbidopa
YUMM
A375
SKMEL2
SH4
SKMEL3
WM46
SKMEL24
WM2664
RPMI-7951

Figure 3.

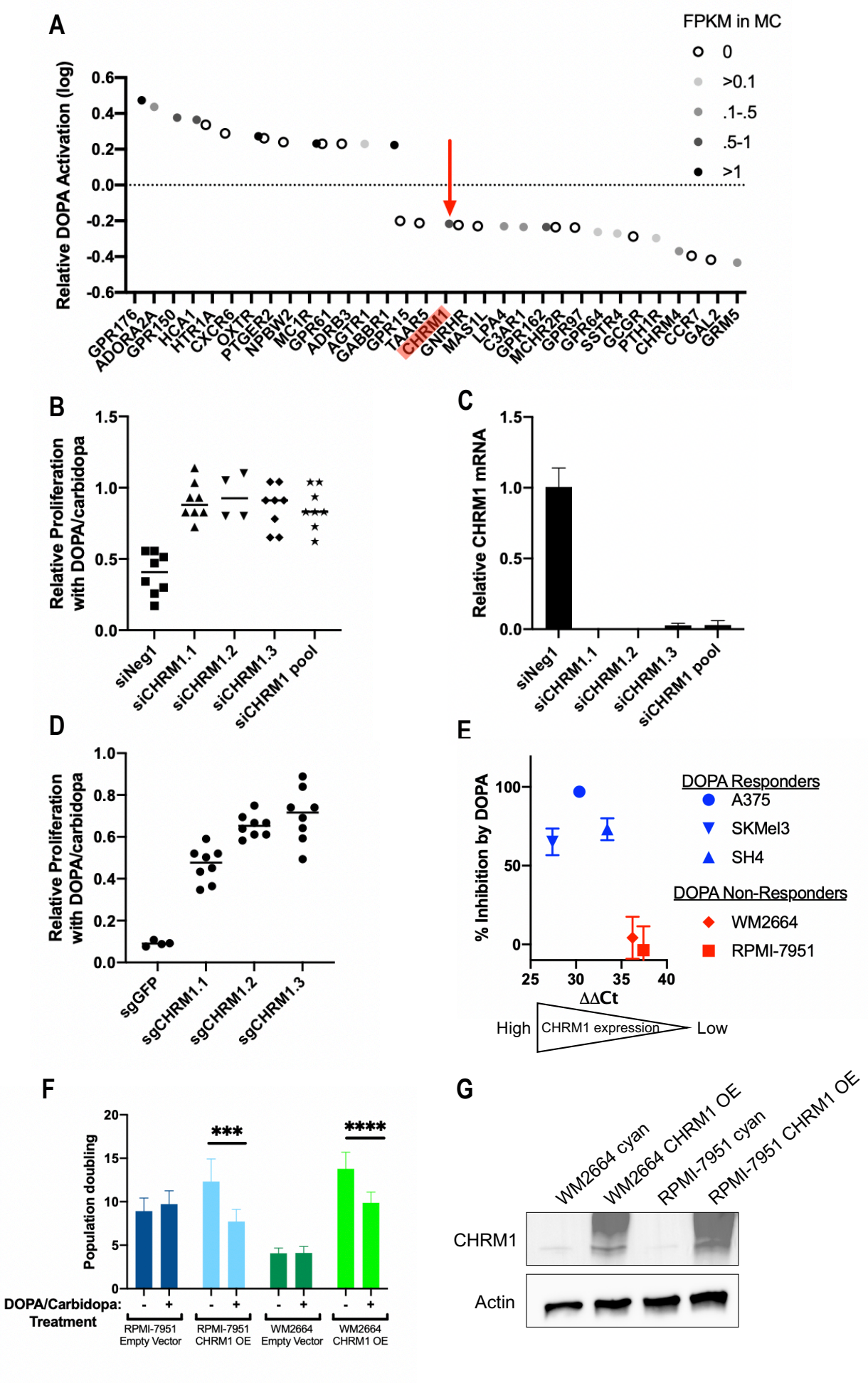
A
FPKM in MC
0
>0.1
.1-.5
.5-1
>1
Relative DOPA Activation (log)
0.6
0.4
0.2
0.0
-0.2
-0.4
-0.6
GPR176
ADORA2A
GPR150
HCA1
HTR1A
CXCR6
OXTR
PTGER2
NPBW2
MC1R
GPR61
ADRB3
AGTR1
GABBR1
GPR15
TAAR5
CHRM1
GNRHR
MAS1L
LPA4
C3AR1
GPR162
MCHR2R
GPR97
GPR64
SSTR4
GCGR
PTH1R
CHRM4
CCR7
GAL2
GRM5
B
Relative Proliferation with DOPA/carbidopa
1.5
1.0
0.5
0.0
siNeg1
siCHRM1.1
siCHRM1.2
siCHRM1.3
siCHRM1 pool
C
Relative CHRM1 mRNA
1.5
1.0
0.5
0.0
siNeg1
siCHRM1.1
siCHRM1.2
siCHRM1.3
siCHRM1 pool
D
Relative Proliferation with DOPA/carbidopa
1.0
0.8
0.6
0.4
0.2
0.0
sgGFP
sgCHRM1.1
sgCHRM1.2
sgCHRM1.3
E
% Inhibition by DOPA
100
50
0
25
30
35
40
ΔΔCt
DOPA Responders
A375
SKMel3
SH4
DOPA Non-Responders
WM2664
RPMI-7951
High
CHRM1 expression
Low
F
Population doubling
20
15
10
5
0
***
****
DOPA/Carbidopa:
Treatment
-
+
RPMI-7951 Empty Vector
RPMI-7951 CHRM1 OE
WM2664 Empty Vector
WM2664 CHRM1 OE
G
WM2664 cyan
WM2664 CHRM1 OE
RPMI-7951 cyan
RPMI-7951 CHRM1 OE
CHRM1
Actin

Figure 4.

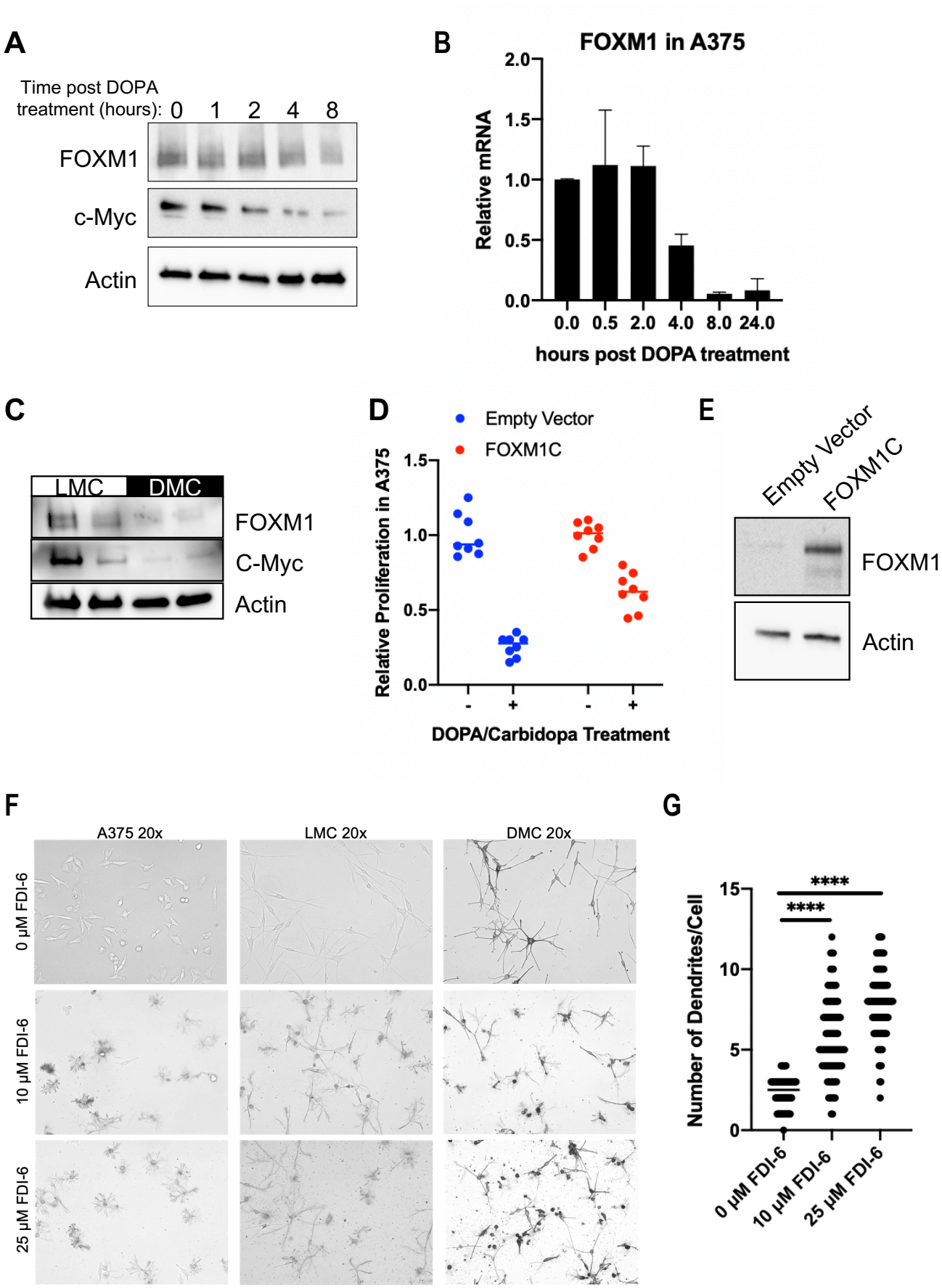
A
Time post DOPA treatment (hours): 0 1 2 4 8
FOXM1
c-Myc
Actin
B
FOXM1 in A375
Relative mRNA
2.0
1.5
1.0
0.5
0.0
0.0 0.5 2.0 4.0 8.0 24.0
hours post DOPA treatment
C
LMC
DMC
FOXM1
C-Myc
Actin
D
Empty Vector
FOXM1C
Relative Proliferation in A375
1.5
1.0
0.5
0.0
- + - +
DOPA/Carbidopa Treatment
E
Empty Vector
FOXM1C
FOXM1
Actin
F
A375 20x
LMC 20x
DMC 20x
0 µM FDI-6
10 µM FDI-6
25 µM FDI-6
G
Number of Dendrites/Cell
15
10
5
0
****
****
0 µM FDI-6
10 µM FDI-6
25 µM FDI-6

Figure 5.

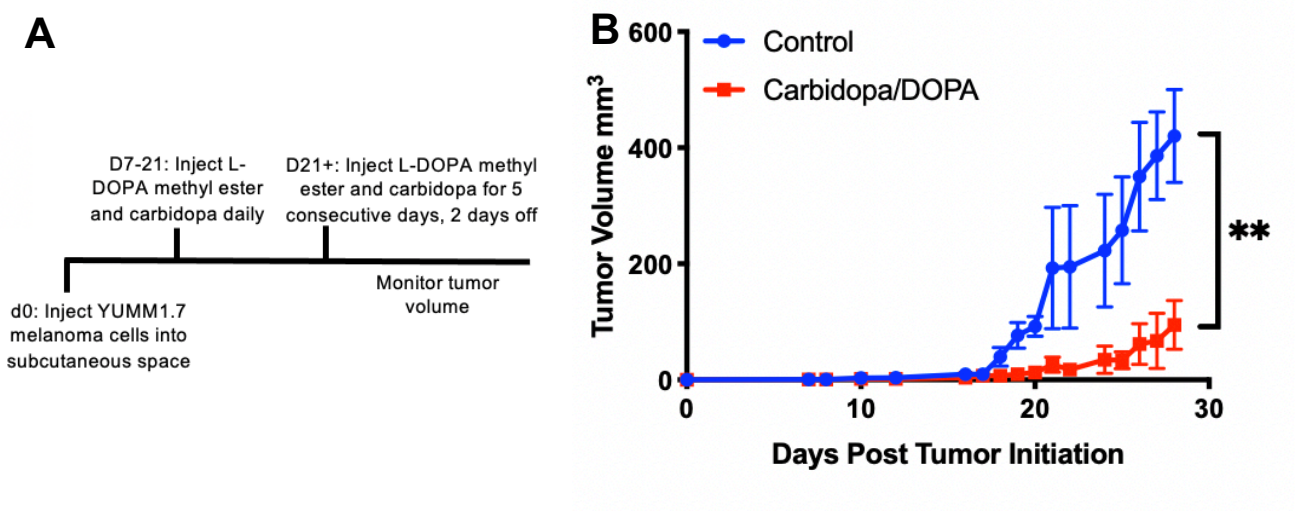
A
D7-21: Inject L-DOPA methyl ester and carbidopa daily
D21+: Inject L-DOPA methyl ester and carbidopa for 5 consecutive days, 2 days off
d0: Inject YUMM1.7 melanoma cells into subcutaneous space
Monitor tumor volume
B
Control
Carbidopa/DOPA
Tumor Volume mm3
600
400
200
0
0
10
20
30
Days Post Tumor Initiation
**

References

1. Hamid, O. *et al.* Safety and tumor responses with lambrolizumab (anti-PD-1) in melanoma. *N. Engl. J. Med.* (2013). doi:10.1056/NEJMoa1305133
2. Ribas, A. *et al.* Association of pembrolizumab with tumor response and survival among patients with advanced melanoma. in *JAMA - Journal of the American Medical Association* (2016). doi:10.1001/jama.2016.4059
3. Cancer Stat Facts: Melanoma of the Skin. *SEER* (2019).
4. Videira, I. F. dos S., Moura, D. F. L. & Magina, S. Mechanisms regulating melanogenesis*. *An. Bras. Dermatol.* (2013). doi:10.1590/s0365-05962013000100009
5. Jimbow, K., Quevedo, W. C., Fitzpatrick, T. B. & Szabo, G. Some aspects of melanin biology: 1950-1975. *J. Invest. Dermatol.* (1976). doi:10.1111/1523-1747.ep12512500
6. Iozumi, K., Hoganson, G. E., Pennella, R., Everett, M. A. & Fuller, B. B. Role of tyrosinase as the determinant of pigmentation in cultured human melanocytes. *J. Invest. Dermatol.* (1993). doi:10.1111/1523-1747.ep12476630
7. Sturm, R. A. Molecular genetics of human pigmentation diversity. *Human Molecular Genetics* (2009). doi:10.1093/hmg/ddp003
8. Kaidbey, K. H., Agin, P. P., Sayre, R. M. & Kligman, A. M. Photoprotection by melanin—a comparison of black and Caucasian skin. *J. Am. Acad. Dermatol.* (1979). doi:10.1016/S0190-9622(79)70018-1
9. Gloster, H. M. & Neal, K. Skin cancer in skin of color. *Ski. Cancer Manag. A Pract. Approach* 217–223 (2010). doi:10.1007/978-0-387-88495-0_16
10. Halder, R. M. & Bang, K. M. Skin Cancer in Blacks in the United States. *Dermatol. Clin.* (1988). doi:10.1016/s0733-8635(18)30651-x
11. Yang, H. M. *et al.* Identification of recurrent mutational events in anorectal melanoma. *Mod. Pathol.* (2017). doi:10.1038/modpathol.2016.179
12. Callahan, A. *et al.* Epidemiology of anorectal melanoma in the United States: 1992 to 2011. *Dermatologic Surg.* (2016). doi:10.1097/DSS.0000000000000579
13. Kiprono, S. K., Chaula, B. M. & Beltraminelli, H. Histological review of skin cancers in African Albinos: A 10-year retrospective review. *BMC Cancer* (2014). doi:10.1186/1471-2407-14-157
14. Mabula, J. B. *et al.* Skin cancers among Albinos at a University teaching hospital in Northwestern Tanzania: a retrospective review of 64 cases. *BMC Dermatol.* (2012). doi:10.1186/1471-5945-12-5
15. Hirobe, T. How are proliferation and differentiation of melanocytes regulated? *Pigment Cell Melanoma Res.* (2011). doi:10.1111/j.1755-148X.2011.00845.x
16. Cichorek, M., Wachulska, M., Stasiewicz, A. & Tymińska, A. Skin melanocytes : biology and development. 30–41 (2013). doi:10.5114/pdia.2013.33376
17. Buac, K. *et al.* NRG1/ERBB3 signaling in melanocyte development and melanoma: Inhibition of differentiation and promotion of proliferation. *Pigment Cell Melanoma Res.* (2009). doi:10.1111/j.1755-148X.2009.00616.x

18. Natale, C. A. *et al.* Sex steroids regulate skin pigmentation through nonclassical membrane-bound receptors. *Elife* (2016). doi:10.7554/elife.15104
19. Natale, C. A. *et al. Non-Classical Estrogen Signaling Inhibits Melanoma and Improves Response to PD-1 Blockade*. *SSRN* (2018). doi:10.2139/ssrn.3155702
20. Suzuki, I., Cone, R. D., Im, S., Nordlund, J. & Abdel-Malek, Z. A. Binding of melanotropic hormones to the melanocortin receptor MC1R on human melanocytes stimulates proliferation and melanogenesis. *Endocrinology* (1996). doi:10.1210/endo.137.5.8612494
21. Valverde, P., Healy, E., Jackson, I., Rees, J. L. & Thody, A. J. Variants of the melanocyte–stimulating hormone receptor gene are associated with red hair and fair skin in humans. *Nature Genetics* (1995). doi:10.1038/ng1195-328
22. Hunt, G., Kyne, S., Wakamatsu, K., Ito, S. & Thody, A. J. Nle4DPhe7α-melanocyte-stimulating hormone increases the eumelanin:phaeomelanin ratio in cultured human melanocytes. *J. Invest. Dermatol.* (1995). doi:10.1111/1523-1747.ep12613565
23. Burchill, S. A., Ito, S. & Thody, A. J. Effects of melanocyte-stimulating hormone on tyrosinase expression and melanin synthesis in hair follicular melanocytes of the mouse. *J. Endocrinol.* (1993). doi:10.1677/joe.0.1370189
24. D'Orazio, J. & Fisher, D. E. Central role for cAMP signaling in pigmentation and UV resistance. *Cell Cycle* (2011). doi:10.4161/cc.10.1.14292
25. Hodgkinson, C. A. *et al.* Mutations at the mouse microphthalmia locus are associated with defects in a gene encoding a novel basic-helix-loop-helix-zipper protein. *Cell* (1993). doi:10.1016/0092-8674(93)90429-T
26. McNeal, A. S. *et al.* CDKN2B loss promotes progression from benign melanocytic nevus to melanoma. *Cancer Discov.* (2015). doi:10.1158/2159-8290.CD-15-0196
27. Chudnovsky, Y., Adams, A. E., Robbins, P. B., Lin, Q. & Khavari, P. A. Use of human tissue to assess the oncogenic activity of melanoma-associated mutations. *Nat. Genet.* (2005). doi:10.1038/ng1586
28. McNeal, A. S. *et al.* CDKN2B loss promotes progression from benign melanocytic nevus to melanoma. *Cancer Discov.* **5**, (2015).
29. Barsh, G. S. What Controls Variation in Human Skin Color? *PLoS Biol.* (2003). doi:10.1371/journal.pbio.0000091
30. Del Marmol, V. & Beermann, F. Tyrosinase and related proteins in mammalian pigmentation. *FEBS Letters* (1996). doi:10.1016/0014-5793(96)00109-3
31. SLOMINSKI, A., MOELLMANN, G. & KUKLINSKA, E. L-Tyrosine, L-DOPA, and Tyrosinase as Positive Regulators of the Subcellular Apparatus of Melanogenesis in Bomirski Ab Amelanotic Melanoma Cells. *Pigment Cell Res.* (1989). doi:10.1111/j.1600-0749.1989.tb00170.x
32. Paschkis, K. E., Cantarow, A., Hart, W. M. & Rakoff, A. E. Inhibitory Action of Thiouracil, Thiocarbamide and Other Compounds on Melanin Formation by Tyrosinase. *Proc. Soc. Exp. Biol. Med.* (1944). doi:10.3181/00379727-57-14690

33. DIEKE, S. H. Pigmentation and hair growth in black rats, as modified by the chronic administration of thiourea, phenyl thiourea and alphanaphthyl thiourea. *Endocrinology* (1947). doi:10.1210/endo-40-3-123
34. Lopez, V. M., Decatur, C. L., Stamer, W. D., Lynch, R. M. & McKay, B. S. L-DOPA is an endogenous ligand for OA1. *PLoS Biol.* (2008). doi:10.1371/journal.pbio.0060236
35. Kroeze, W. K. *et al.* PRESTO-Tango as an open-source resource for interrogation of the druggable human GPCRome. *Nat. Struct. Mol. Biol.* (2015). doi:10.1038/nsmb.3014
36. Baig, A. M. *et al.* Differential receptor dependencies: Expression and significance of muscarinic M1 receptors in the biology of prostate cancer. *Anticancer. Drugs* (2017). doi:10.1097/CAD.0000000000000432
37. Magnon, C. *et al.* Autonomic nerve development contributes to prostate cancer progression. *Science (80-.).* (2013). doi:10.1126/science.1236361
38. Yin, Q. Q., Xu, L. H., Zhang, M. & Xu, C. Muscarinic acetylcholine receptor M1 mediates prostate cancer cell migration and invasion through hedgehog signaling. *Asian J. Androl.* (2018). doi:10.4103/aja.aja_55_18
39. Buchli, R., Ndoye, A., Arredondo, J., Webber, R. J. & Grando, S. A. Identification and characterization of muscarinic acetylcholine receptor subtypes expressed in human skin melanocytes. *Mol. Cell. Biochem.* (2001). doi:10.1023/A:1013368509855
40. Hammer, R., Berrie, C. P., Birdsall, N. J. M., Burgen, A. S. V. & Hulme, E. C. Pirenzepine distinguishes between different subclasses of muscarinic receptors [28]. *Nature* (1980). doi:10.1038/283090a0
41. Blum, A. L. & Hammer, R. DIE BEHANDLUNG DES ULCUS PEPTICUM MIT PIRENZEPIN. (1979).
42. Langley, J. N. On the Physiology of the Salivary Secretion: Part II. On the Mutual Antagonism of Atropin and Pilocarpin, having especial reference to their relations in the Sub-maxillary Gland of the Cat. *J. Physiol.* (1878). doi:10.1113/jphysiol.1878.sp000028
43. Pronin, A. N., Wang, Q. & Slepak, V. Z. Teaching an old drug new tricks: Agonism, antagonism, and biased signaling of pilocarpine through M3 muscarinic acetylcholine receptor. *Mol. Pharmacol.* (2017). doi:10.1124/mol.117.109678
44. Murga, C., Laguinge, L., Wetzker, R., Cuadrado, A. & Gutkind, J. S. Activation of Akt/Protein Kinase B by G Protein-coupled Receptors. *J. Biol. Chem.* (1998). doi:10.1074/jbc.273.30.19080
45. Goldsmith, Z. G. & Dhanasekaran, D. N. G Protein regulation of MAPK networks. *Oncogene* (2007). doi:10.1038/sj.onc.1210407
46. Brose, M. S. *et al.* BRAF and RAS mutations in human lung cancer and melanoma. *Cancer Res.* (2002).
47. Davies, H. *et al.* Mutations of the BRAF gene in human cancer. *Nature* (2002). doi:10.1038/nature00766
48. Slipicevic, A. *et al.* Expression of activated Akt and PTEN in malignant Melanomas: Relationship with clinical outcome. *Am. J. Clin. Pathol.* (2005). doi:10.1309/YT58WWMTA6YR1PRV
49. Fecher, L. A., Amaravadi, R. K. & Flaherty, K. T. The MAPK pathway in melanoma. *Current Opinion in Oncology* (2008). doi:10.1097/CCO.0b013e3282f5271c
50. Wang, Z. *et al.* Down-regulation of Notch-1 is associated with Akt and FoxM1 in inducing cell growth

inhibition and apoptosis in prostate cancer cells. *Journal of Cellular Biochemistry* (2011). doi:10.1002/jcb.22770

51. Miyashita, A. *et al.* Investigation of FOXM1 as a Potential New Target for Melanoma. *PLoS One* (2015). doi:10.1371/journal.pone.0144241
52. Bonet, C. *et al.* Aurora B is regulated by the mitogen-activated protein kinase/extracellular signal-regulated kinase (MAPK/ERK) signaling pathway and is a valuable potential target in melanoma cells. *J. Biol. Chem.* (2012). doi:10.1074/jbc.M112.371682
53. Wang, X., Kiyokawa, H., Dennewitz, M. B. & Costa, R. H. The forkhead box m1b transcription factor is essential for hepatocyte DNA replication and mitosis during mouse liver regeneration. *Proc. Natl. Acad. Sci. U. S. A.* (2002). doi:10.1073/pnas.252570299
54. Wonsey, D. R. & Follettie, M. T. Loss of the forkhead transcription factor FoxM1 causes centrosome amplification and mitotic catastrophe. *Cancer Res.* (2005). doi:10.1158/0008-5472.CAN-04-4059
55. Ito, T. *et al.* Prognostic significance of forkhead box M1 (FoxM1) expression and antitumour effect of FoxM1 inhibition in melanoma. *Histopathology* (2016). doi:10.1111/his.12909
56. Liao, G. Bin *et al.* Regulation of the master regulator FOXM1 in cancer. *Cell Communication and Signaling* (2018). doi:10.1186/s12964-018-0266-6
57. Gormally, M. V. *et al.* Suppression of the FOXM1 transcriptional programme via novel small molecule inhibition. *Nat. Commun.* (2014). doi:10.1038/ncomms6165
58. Rousseau, K. *et al.* Proopiomelanocortin (POMC), the ACTH/melanocortin precursor, is secreted by human epidermal keratinocytes and melanocytes and stimulates melanogenesis. *FASEB J.* (2007). doi:10.1096/fj.06-7398com
59. Herlyn, M., Mancianti, M. L., Jambrosic, J., Bolen, J. B. & Koprowski, H. Regulatory factors that determine growth and phenotype of normal human melanocytes. *Exp. Cell Res.* (1988). doi:10.1016/0014-4827(88)90271-6
60. Marsden, C. D., Parkes, J. D. & Rees, J. E. A YEAR'S COMPARISON OF TREATMENT OF PATIENTS WITH PARKINSON'S DISEASE WITH LEVODOPA COMBINED WITH CARBIDOPA VERSUS TREATMENT WITH LEVODOPA ALONE. *Lancet* (1973). doi:10.1016/S0140-6736(73)92729-3
61. Slominski, A. & Daniel, P. L-Dopa binding sites in rodent melanoma cells. *BBA - Mol. Basis Dis.* (1992). doi:10.1016/0925-4439(92)90109-Z
62. Slominski, A. & Paus, R. Towards defining receptors for l-tyrosine and l-DOPA. *Mol. Cell. Endocrinol.* **99**, 1987–1991 (1994).
63. Slominski, A., Zmijewski, M. A. & Pawelek, J. L-tyrosine and L-dihydroxyphenylalanine as hormone-like regulators of melanocyte functions. *Pigment Cell and Melanoma Research* (2012). doi:10.1111/j.1755-148X.2011.00898.x
64. Slominski, A. & Paus, R. Are L-tyrosine and L-dopa hormone-like bioregulators? *J. Theor. Biol.* (1990). doi:10.1016/S0022-5193(05)80292-9
65. Wick, M. M., Byers, L. & Frei, E. L-dopa: Selective toxicity for melanoma cells in vitro. *Science (80-.).*

(1977). doi:10.1126/science.877570

66. Wick, M. M. Levodopa and Dopamine Analogs as DNA Polymerase Inhibitors and Antitumor Agents in Human Melanoma. *Cancer Res.* (1980).
67. Wick, M. M., Kramer, R. A. & Gorman, M. Enhancement of L-dopa incorporation into melanoma by dopa decarboxylase inhibition. *J. Invest. Dermatol.* (1978). doi:10.1111/1523-1747.ep12543559
68. Wick, M. M. L-Dopa methyl ester as a new antitumour agent. *Nature* (1977). doi:10.1038/269512a0
69. Wick, M., Byers, L. & Frei, E. 3rd. L-dopa: selective toxicity for melanoma cells in vitro. *Science (80-.).* **197**, 468–9
70. Wick, M., Byers, L. & Ratliff, J. Selective toxicity of 6-hydroxydopa for melanoma cells. *J. Invest. Dermatol.* **72**, 67–9
71. Chua, W. H. *et al.* Atropine for the Treatment of Childhood Myopia. *Ophthalmology* (2006). doi:10.1016/j.ophtha.2006.05.062
72. Spinks, A. & Wasiak, J. Scopolamine (hyoscine) for preventing and treating motion sickness. *Cochrane Database Syst. Rev.* (2011). doi:10.1002/14651858.cd002851.pub4
73. Hara, M. *et al.* Innervation of melanocytes in human skin. *J. Exp. Med.* (1996). doi:10.1084/jem.184.4.1385
74. Poewe, W. *et al.* Parkinson disease. *Nat. Rev. Dis. Prim.* (2017). doi:10.1038/nrdp.2017.13
75. Dalvin, L. A., Damento, G. M., Yawn, B. P., Abbott, B. A. & Pulido, J. S. Parkinsons disease and melanoma: confirming and reexamining an association. *Pigment cell melanoma Res. Conf. 27th Annu. Meet. japanese Soc. Pigment cell Res. Japan. Conf. start 20161112. Conf. end 20161113* (2017).
76. Olsen, J. H. *et al.* Atypical cancer pattern in patients with Parkinson's disease. *Br. J. Cancer* (2005). doi:10.1038/sj.bjc.6602279
77. Olsen, J. H., Friis, S. & Frederiksen, K. Malignant melanoma and other types of cancer preceding parkinson disease. *Epidemiology* (2006). doi:10.1097/01.ede.0000229445.90471.5e
78. Dahodwala, N. *et al.* Racial differences in the diagnosis of Parkinson's disease. *Mov. Disord.* (2009). doi:10.1002/mds.22557
79. Kessler, I. I. Epidemiologic studies of parkinson's disease: II. A hospital-based survey. *Am. J. Epidemiol.* (1972). doi:10.1093/oxfordjournals.aje.a121399
80. Kessler, I. I. Epidemiologic studies of parkinson's disease: III. A community-based survey. *Am. J. Epidemiol.* (1972). doi:10.1093/oxfordjournals.aje.a121455
81. Raychaudhuri, P. & Park, H. J. FoxM1: A master regulator of tumor metastasis. *Cancer Research* (2011). doi:10.1158/0008-5472.CAN-11-0640
82. Ziegler, Y. *et al.* Suppression of FOXM1 activities and breast cancer growth in vitro and in vivo by a new class of compounds. *npj Breast Cancer* (2019). doi:10.1038/s41523-019-0141-7
83. Natale, C. A. *et al.* Activation of G protein-coupled estrogen receptor signaling inhibits melanoma and improves response to immune checkpoint blockade. *Elife* (2018). doi:10.7554/elife.31770
84. Duperret, E. K., Dahal, A. & Ridky, T. W. Focal-adhesion-independent integrin-av regulation of FAK and

c-Myc is necessary for 3D skin formation and tumor invasion. *J. Cell Sci.* **128**, (2015).

85. Duperret, E. K., Natale, C. A., Monteleon, C., Dahal, A. & Ridky, T. W. The integrin αv-TGFβ signaling axis is necessary for epidermal proliferation during cutaneous wound healing. *Cell Cycle* (2016). doi:10.1080/15384101.2016.1199306
86. Djaldetti, R., Atlas, D. & Melamed, E. Effect of subcutaneous administration of levodopa ethyl ester, a soluble prodrug of levodopa, on dopamine metabolism in rodent striatum: Implication for treatment of Parkinson's disease. *Clin. Neuropharmacol.* (1996). doi:10.1097/00002826-199619010-00005
87. Meadows, G. G., Pierson, H. F., Abdallah, R. M. & Desai, P. R. Dietary Influence of Tyrosine and Phenylalanine on the Response of B16 Melanoma to Carbidopa-Levodopa Methyl Ester Chemotherapy. *Cancer Res.* (1982).
88. Natale, C. A. C. A. *et al.* Sex steroids regulate skin pigmentation through nonclassical membrane-bound receptors. *Elife* **5**, (2016).